JOURNAL OF Applied Polymer SCIENCE

Laser Scanning Confocal Microscopy Versus Scanning Electron Microscopy for Characterization of Polymer Morphology: Sample Preparation Drastically Distorts Morphologies of Poly(2-hydroxyethyl methacrylate)-Based Hydrogels

Stefan M. Paterson,[1] Ylenia S. Casadio,[1] David H. Brown,[1,2] Jeremy A. Shaw,[3] Traian V. Chirila,[4,5,6,7] Murray V. Baker[1,4]

[1]School of Chemistry and Biochemistry M313, The University of Western Australia, Crawley, W.A. 6009, Australia
[2]Nanochemistry Research Institute, Department of Chemistry, Curtin University of Technology, Kent St, Bentley, W.A. 6102, Australia
[3]Centre for Microscopy, Characterisation and Analysis, The University of Western Australia, Crawley, WA 6009, Australia
[4]Queensland Eye Institute, 41 Annerley Road, South Brisbane, Queensland 4101, Australia
[5]Faculty of Science and Technology, Queensland University of Technology, Brisbane, Queensland 4001, Australia
[6]Australian Institute for Bioengineering and Nanotechnology, University of Queensland, St Lucia, Queensland 4072, Australia
[7]Faculty of Health Science, University of Queensland, Herston, Queensland 4006, Australia
Correspondence to: M. V. Baker (E-mail: murray.baker@uwa.edu.au)

ABSTRACT: The internal morphologies for a series of heterogeneous PHEMA and P[HEMA-*co*-MeO-PEGMA] [PHEMA = poly(2-hydroxyethyl methacrylate), MeO-PEGMA = poly(ethylene glycol) methyl ether methacrylate] hydrogels were characterized by scanning electron microscopy (SEM) in conjunction with a sample drying procedure, and by laser scanning confocal microscopy (LSCM) without prior drying. Compared to SEM, LSCM was far simpler and more rapid technique for imaging hydrogels. LSCM also allowed the native hydrated morphology of the hydrogels to be characterized, whereas SEM could only characterize the morphology of samples in their dehydrated state. No dehydration method used in this study preserved the true native morphology, but plunge freezing/freeze drying was the most suitable method that best preserved the native morphology for all hydrogel compositions. Refrigerated freezing/freeze-drying and critical point drying introduced significant morphological artifacts, the severity of the artifacts being dependant on the sample's composition and *Tg*. © 2012 Wiley Periodicals, Inc. J. Appl. Polym. Sci. 000: 000–000, 2012

KEYWORDS: hydrogels; macroporous polymers; morphology; poly(2-hydroxyethyl methacrylate); laser scanning confocal microscopy

Received 1 March 2012; accepted 8 May 2012; published online
DOI: 10.1002/app.38034

INTRODUCTION

Hydrogels based on poly(2-hydroxyethyl methacrylate) (PHEMA) (Scheme 1) are highly biocompatible and have a long history of applications in the biomedical field.[1] PHEMA-based hydrogel sponges are potential candidates for uses as tissue engineering scaffolds. They have already found clinical application in an artificial cornea,[2] and have potential for applications as scaffolds for neural regeneration[3–7] and as a component of an orbital enucleation implant.[8] PHEMA-based hydrogel sponges can be easily synthesized by a method known as polymerization-induced phase separation.[9] Sponges formed in this way have a morphology based on numerous "connected droplets," and the spaces between these droplets form a network of interconnected pores.[9] A requirement for the use of these sponges as scaffolds in tissue engineering is that the dimensions of the pores are suitable to allow cellular infiltration.[10–15] Thus, it is important that the morphology of hydrogel scaffolds can be characterized reliably.

Ideally, a hydrogel scaffold should be characterized in its hydrated form. Techniques such as cryo-scanning electron microscopy (cryo-SEM) allow imaging of frozen hydrated samples, but these techniques are not always readily available and the procedures for sample preparation and imaging can be time consuming. Laser scanning confocal microscopy (LSCM) offers an alternative method for characterization and has been used to characterize poly(vinyl alcohol) hydrogels,[16] and more recently poly(*N*-isopropyl acrylamide)[17] and poly(2-hydroxyethyl

Additional Supporting Information may be found in the online version of this article.

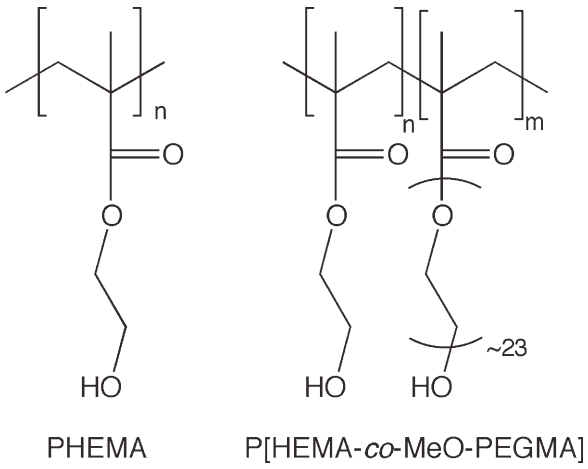

Scheme 1. Molecular structures of PHEMA and P[HEMA-*co*-MeO-PEGMA] hydrogels.

methacrylate-L-lactide-dextran) hydrogels.[18] LSCM uses a dye that is excited by light (generally from a laser source), and then emits red-shifted light that is detected and used to construct an image. For PHEMA-based hydrogels to be imaged using LSCM, the hydrogels must first be labeled with a fluorescent dye. As both labeling and imaging can be carried out in aqueous environments that are close to physiological conditions, no dehydration of the hydrogels is required, thereby avoiding the possibility of introduction of artifacts by drying procedures. For hydrogels based on PHEMA, labeling does not require special equipment or unusual experimental skills, and is a relatively trivial step in the characterization procedure.

Despite the obvious applicability of LSCM to imaging of hydrogels, SEM is the most established method for characterization of the morphologies of hydrogels because of its ability to resolve structures in sufficient detail[9,13,19] and its relatively long history of use. A significant issue in the characterization of hydrogels by SEM is sample preparation. Before a hydrogel can be imaged by SEM, it must be dried and then it must be rendered conductive by the deposition of a thin layer of carbon and/or gold or platinum. The removal of water from the hydrogel must be done in such a way as to preserve as far as possible the morphology of the hydrated sample. The matter is further complicated because hydrogels are, by definition, very hydrophilic materials that are able to absorb many times their own weight in water. Consequently, dehydration processes can have profound effects on the morphology of hydrogels.[20,21] In addition, hydrogels, as materials, fall between a biological and a traditional hard material sample, with the knowledge of how hydrogels behave during sample preparation procedures being considerably less than that of biological and/or hard materials. Nonetheless, two common methods used to dehydrate hydrogels prior to SEM are freeze-drying[21,22] and critical point drying.[9,21,23,24] Even though freeze-drying and critical point drying are used extensively to prepare samples for SEM,[13,19] few articles adequately explain the drying protocols, with the impact of these techniques on the native morphology of hydrogels having only been partially researched.[20] The problems associated with freeze-drying and critical point drying are detailed below.

In freeze-drying, the sample is cooled (frozen) so that the water within becomes ice, and then dehydration is achieved by sublimation of ice under reduced pressure. Freezing can be achieved by various methods, and the liquid water can pass into the solid phase to form either crystalline or non-crystalline (vitreous) ice.[25] Ideally, freezing should be rapid and result in the formation of vitreous ice, because the growth of ice crystals, which form if the rate of freezing is too slow, can cause damage to the sample. Conversely, if a sample containing vitreous ice is allowed to warm, the ice will once again crystallize or devitrify. Freeze-drying aims to remove water (by sublimation of ice) before these changes in phase occur.[26]

In critical point drying, water in the sample is replaced by a transitional fluid, such as acetone, which is in turn replaced by liquid CO2, and the sample is then heated to the temperature at which CO2 becomes supercritical (ca., 31°C). If the temperature required to reach supercritical conditions is above the glass transition point (Tg) of the hydrogel, the hydrogel may "melt" and the native pore morphology will be distorted or destroyed.[20,21]

In a recent study of some P[HEMA-*co*-MeO-PEGMA] hydrogels (Scheme 1), we found that the morphology of the hydrogel, as revealed by SEM, depended on the method used to dry the sample prior to SEM, with freeze-drying and critical point drying resulting in vastly different morphologies[21]; other researches have also discovered this problem for poly(vinyl alcohol) hydrogels.[20] This result raised the question of which dehydration method minimizes distortion or the introduction of other more pronounced experimental artifacts in a hydrogel sample, and thus allows SEM to provide the most accurate representation of the hydrogel's native morphology. In this article, we address this question by comparing the morphologies of hydrated PHEMA and P[HEMA-*co*-MeO-PEGMA] gels and sponges, as revealed by LSCM, with the morphologies of the corresponding dehydrated hydrogels, as revealed by SEM.

MATERIALS AND METHODS

Materials

2-Hydroxyethyl methacrylate (HEMA) (Bimax, Glen Rock, PA, USA, > 99.0%) was distilled (b.p. 38–39°C/0.1 mmHg) and stored at −20°C prior to use. Tetra(ethylene glycol) dimethacrylate (TEGDMA) (Fluka, Sigma-Aldrich, St Louis, MO, USA), 2,2-dimethoxy-2-phenylacetophenone (DPAP) (Irgacure 651, Aldrich, 97%), sodium chloride (Fluka, AR grade), fluorescein isothiocyanate (Aldrich), and rhodamine B isothiocyanate (Aldrich) were all used as received. Poly(ethylene glycol) methyl ether methacrylate (MeO-PEGMA) (Aldrich, M_n ca., 1100) was recrystallized from hot ether to remove the inhibitor.

Preparation of Hydrogels

Polymer hydrogels were prepared as described previously[21] by photoinitiated polymerization of HEMA or HEMA/MeO-PEGMA mixtures in water or 0.8*M* NaCl, using the formulations summarized in Table I. All polymerizations were initiated using DPAP (0.1 mol % with respect to HEMA) under a UV lamp (UVP, Upland, CA, Blak-Ray®, 365 nm, 120 W) for 30 min. TEGDMA was used as a crosslinking agent at 1 mol % with respect to HEMA. After polymerization, the hydrogels were soaked in water for 1 week to remove any unreacted monomers, with water being exchanged daily. After

Table I. Formulations of PHEMA-Based Hydrogels

Formulation	H_2O : HEMA : MeO-PEGMA[a]	[NaCl][b]	Macroscopic appearance
1	80 : 20 : 0	-	White
2	80 : 20 : 2	0.8*M*	White
3	80 : 20 : 5	-	Transparent
4	80 : 20 : 5	0.8*M*	White
5	80 : 20 : 8	-	Transparent
6	80 : 20 : 8	0.8*M*	White

[a]The copolymers are identified based on the ratio A : B : C for the polymerization mixture, where A = part by weight water or 0.8*M* NaCl, B = part by weight HEMA, C = part by weight MeO-PEGMA.
[b]For formulations 2, 4, and 6, 0.8*M* NaCl was used in place of H_2O.

soaking, all polymer samples were cut into 300 μm thick cross-sections (Vibratome, 3000, Wetzlar, Germany) and these sections were further cut into disks using a 5 mm biopsy cutter. After sectioning, the samples were carefully transferred by soft plastic tweezers into vials of deionized water, where they were stored until required.

Methods for Dehydration of Samples Prior to Analysis by SEM

Refrigerated Freezing and Freeze-Drying. Refrigerated freezing (Hingham, MA) was carried out by placing hydrogel samples in a conventional freezer at −20°C until frozen. Samples were then freeze-dried (Dynavac FD2, Hingham, MA) until a constant mass was reached.

Plunge-Freezing/Freeze-Drying. Plunge-freezing was performed by plunging hydrogel samples, delicately placed at the tip of a clean spatula, into liquid nitrogen (LN2). Once frozen, all samples were stored in LN2. Low-temperature freeze-drying was carried out using a LN2 cooled turbo freeze-dryer (Emitech, K775X, Quorum Technologies, Ashford, UK). During the transfer from LN2 storage to the freeze-dryer chamber, special care was taken to ensure that samples were immersed in LN2 at all times. The freeze-drying process occurred under vacuum (ca., 7×10^{-5} torr) and during the process the sample was gradually warmed according to the following protocol: held at −120°C for 2 h, increased to −75°C over 1.5 h, held at −75°C for 1 h, increased to 20°C over 5 h.

Critical Point Drying. Hydrated polymer samples were soaked in acetone (ca., 2 mL) for at least 3 h before being placed in the critical point drying apparatus (Emitech, K850). The samples were flushed three or four times with liquid CO_2 to remove the acetone and to ensure complete permeation of CO_2 liquid throughout the sample. The sample chamber was then slowly heated to a value between 35 and 37°C to achieve supercritical conditions, after which the sample chamber was slowly vented. While the sample chamber was vented, a temperature above 31.1°C was maintained to prevent the re-condensation of liquid CO_2.

Scanning Electron Microscopy

Dehydrated samples were mounted on double-sided carbon tabs and coated with a layer of carbon (∼ 30 nm thick) using a carbon evaporator (Speedivac 12E6/1178, Edwards High Vacuum LTD, Crawley, UK). The samples were then imaged by SEM (Zeiss, Berlin, Germany, 1555 VF-FESEM) at 3 kV, using a working distance of 6 mm and an aperture of 10 μm. To acquire an image, frame integration was used to prevent charging on the surface of the polymer.

Labeling Hydrogels for Laser Scanning Confocal Microscopy

Hydrogel samples were soaked in a 0.05% w/v aqueous solution of either fluorescein isothiocyanate (FITC) or rhodamine B isothiocyanate (RBITC) for 24 h at 37°C to functionalize the hydroxyl groups of some HEMA repeat units. To remove excess FITC or RBITC, the samples were rinsed at 4°C in Millipore, Billerica, MA, water for 48 h, during which the water was replaced with fresh water every 12 h. This operation was done in the dark to prevent photobleaching of the dyes, and when rinsing was complete, the samples were stored in the dark at 4°C.

Imaging by LCSM was carried out at room temperature using a multiphoton confocal microscope (Leica, Wetzlar, Germany, TCS SP2 AOBS) with a resolution of 1024 × 1024 pixels, a 20× dry objective using a 458 nm Ar/Kr laser for FITC excitation or a 561 nm red neon laser for RBITC excitation. The labeled polymers were placed onto a 170-μm thick cover slip and any excess water surrounding the polymer was carefully blotted away before the sample was placed into the instrument.

RESULTS AND DISCUSSION

PHEMA-Based Hydrogels

PHEMA hydrogels can have a pore morphology that can either be classified as homogeneous or heterogeneous. Homogeneous PHEMA hydrogels have a pore size in the range of 10–100 nm, are transparent in appearance, and are classified as gels. Heterogeneous PHEMA hydrogels are generally obtained from solution polymerization, are transparent to opaque in appearance, and have pores ranging from 100 nm to 1 μm.[9] When a diluent is used in concentrations greater than 45% w/w, polymerization-induced phase separation occurs and produces PHEMA hydrogels that have pores larger than 1 μm.[9] PHEMA hydrogels produced by this method are more commonly referred to as sponges as they have an interconnected pore morphology and are opaque white in macroscopic appearance. If the hydrophilicity of the PHEMA polymer chains is changed, such as by the inclusion of the hydrophilic monomer MeO-PEGMA, then phase separation is suppressed and the resulting polymer will be a homogenous PHEMA gel, even at high diluent concentrations. In these situations, if the ionic strength of the polymerization solution is increased through the addition of salts, such as NaCl, the solubility of the growing polymer will be reduced and the polymer will precipitate out of solution forming a hydrogel sponge.[21]

Based on the above, a series of hydrogels was prepared by varying the monomer composition and the ionic strength of the polymerization mixture. The hydrogel samples included opaque PHEMA and P[HEMA-*co*-MeO-PEGMA] sponges and transparent P[HEMA-*co*-MeO-PEGMA] gels (Table I).

Imaging PHEMA Sponges

Laser Scanning Confocal Microscopy. LSCM images for hydrated 80 : 20 PHEMA sponges are shown in Figure 1(a,b). The images reveal a morphology based on polymer droplets of 3–4 μm in diameter, typical of a PHEMA sponge.[9] The dye used (FITC or RBITC) does not noticeably affect the quality of the LSCM image. The dyeing process involved the samples being soaked in an aqueous solution of the appropriate dye for 24 h,

Applied Polymer SCIENCE

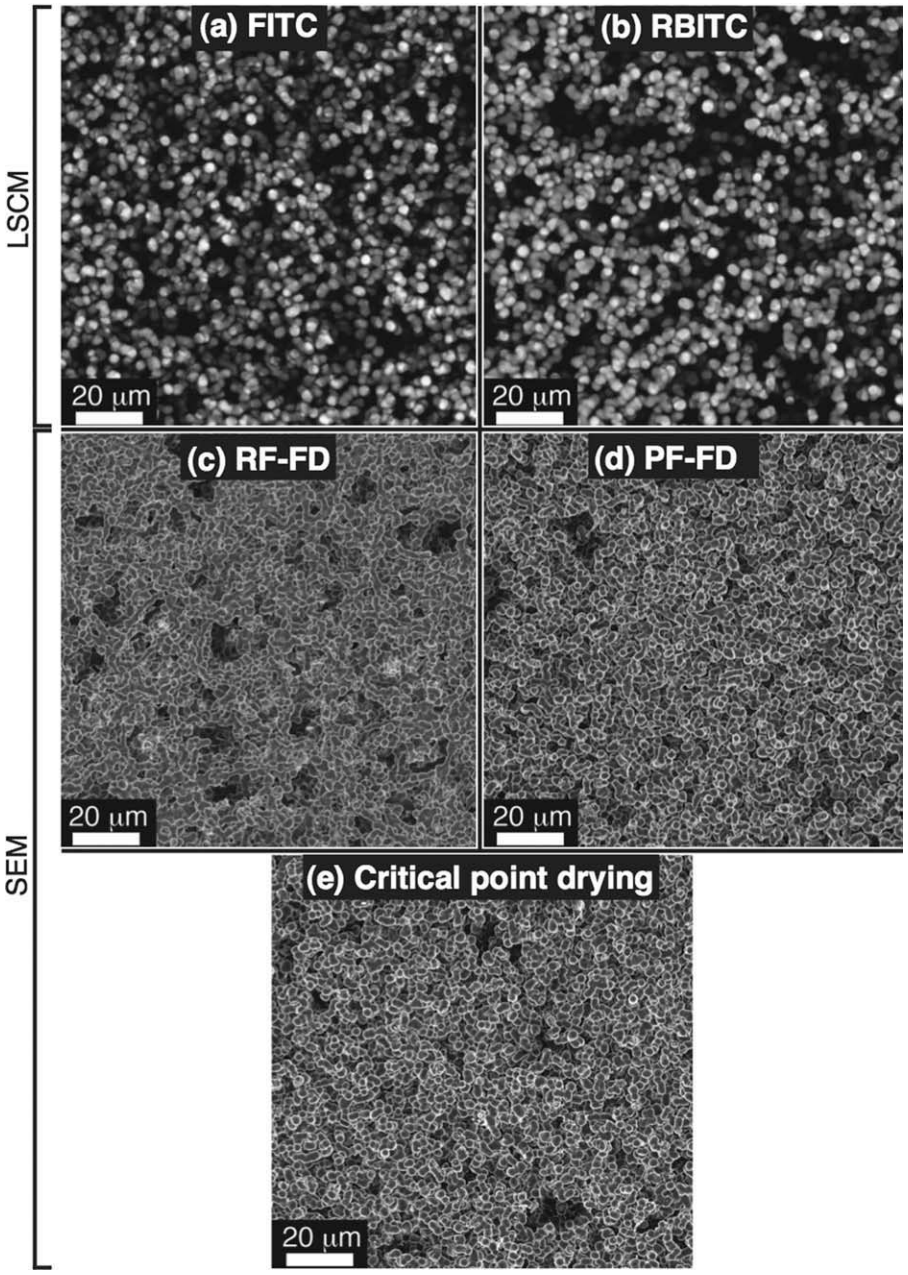

Figure 1. LSCM and SEM images of 80 : 20 H2O : HEMA sponge specimens prepared for microscopy by either labeling (with FITC or RBITC) or by dehydration (using RF-FD, PF-FD, or critical point drying). Colored LSCM images can be viewed in the Supporting Information Figure S1.

and then excess dye being washed away by soaking samples in deionized water for 48 h, replacing the water every 6–12 h. The samples remained hydrated throughout the staining, rinsing, and imaging processes, and so we believe that the morphology seen in the LSCM images accurately reflects the native morphology of the sponges. The time required to image each sample (ca., 2–5 min) was less than the time at which the dyes begin to photobleach, usually after 10 min of imaging. Once the dyes began to bleach, the quality and clarity of the images decreased rapidly, but generally FITC tended to bleach slightly faster than RBITC.

Scanning Electron Microscopy. SEM images of PHEMA sponges (Entry 1, Table I) that were dehydrated by refrigerated freeze/freeze-drying (RF-FD) showed some differences in morphology compared to samples imaged by LSCM. The morphology seen in SEM images showed droplets of 2–3 μm in diameter, but most of the droplets show significant distortion from spherical shape and partial coalescence to neighboring droplets [Figure 1(c)]. In addition, the image shows numerous narrow pores of dimensions of the order of 10 μm, which may have resulted from the expansion of water ice formed during the relatively slow refrigerated freezing process. During this process, ice crystals presumably grew unchecked as the sample cooled to -20°C over 20–30 min. While we appreciate that RF-FD may be considered a "crude" preparation method compared to other more specialized dehydration methods, the inclusion of RF-FD

in this study was to demonstrate the high levels of morphological distortion that can result during sample preparation procedures.

When samples were dehydrated using either plunge freeze/freeze-drying (PF-FD) [Figure 1(d)] or critical point drying [Figure 1(e)], the SEM images showed morphologies of polymer droplets of 2–3 μm, and again the droplets showed distortion from spherical shape and partial coalescence, but the extent of the distortion was less than seen for RF-FD samples, with samples subjected to critical point drying showing the least distortion. There were few significant pores seen in samples dried by PF-FD or critical point drying. Plunge freezing in liquid nitrogen (used in PF-FD) is expected to result in the formation of only small ice crystals, where the dimensions of the ice crystals would be considerably smaller (i.e., nm scales) than the dimensions of the pore features (i.e., μm scales), and so large pores resulting from unchecked growth of water ice would be expected to be reduced compared to the RF-FD case. Although freezing in liquid nitrogen may not provide sufficiently rapid cooling to guarantee formation of vitreous ice throughout large samples, the rate of cooling should be sufficient for formation of vitreous ice in the outer few tens of microns, thus preserving the macro-scale surface morphology of the sample. Thus, the surface of the specimen—as imaged by SEM—should closely match the native morphology. Critical point drying does not rely on freezing of the sample, and so the formation of pores due to ice crystals is not an issue. Deformation of the morphology of samples subjected to critical point drying due to thermal effects is also not expected, since the *Tg* of PHEMA sponges (119°C) is well above the temperature needed to achieve supercritical conditions.[21] It is possible that, during the critical point drying procedure, immersion of samples in acetone results in changes in the swollen state of the hydrogels that could lead to artifacts in the SEM images. Figure 1(e) suggests that such artifacts, if they arise, are small.

These results demonstrate that, while PF-FD or critical point drying of PHEMA hydrogel sponges for SEM more closely preserves the native morphology compared to RF-FD, some distortion of hydrogel morphology is apparent when compared to LSCM. The reduction in droplet size seen in SEM images compared to LSCM images is doubtless a consequence of shrinkage of samples during the drying process (the thickness and diameter of the disks of 80 : 20 PHEMA sponges typically shrank by 20%, regardless of the method used). The apparent coalescence of droplets seen in SEM images may be an artifact of dehydration, or the result of lower image resolution offered in LSCM compared to SEM. Importantly, it appears that LSCM of hydrated samples (which do not need to be dried) facilitates qualitative and quantitative observations and measurements of material that can be considered as being in its "native state." Additionally, LSCM provides a more realistic cross-section of the "true" morphology of PHEMA sponges as a result of a narrower depth of field when compared to SEM. These results provide the clearest indication of sponge morphology for wet scaffold applications.

Imaging P[HEMA-*co*-MeO-PEGMA] Heterogeneous Sponges

As the proportion of MeO-PEGMA in the P[HEMA-*co*-MeO-PEGMA] hydrogels increases, the hydrophilicity of the polymer is increased and consequently phase separation during polymerization is increasingly suppressed. To force phase separation polymerization (and in doing so attain polymers having the desirable droplet morphology), the polymerizations were conducted in 0.8*M* NaCl solutions. An increase in the proportion of MeO-PEGMA in P[HEMA-*co*-MeO-PEGMA] hydrogels results in a decrease in *Tg*.[21]

Laser Scanning Confocal Microscopy. When confocal microscopy was used to image the P[HEMA-*co*-MeO-PEGMA] hydrogels with a composition of 80 : 20 : 2 [Figure 2(a,d)], 80 : 20 : 5 [Figure 2(b,e)], and 80 : 20 : 8 [Figure 2(c,f)], the morphologies seen were comparable to the morphologies seen by LSCM for PHEMA sponges [Figure 1(a,b)]. The morphologies were based on droplets of about 4–5 μm in diameter, with droplets being larger for sponges with higher MeO-PEGMA content. When RBITC was used as a dye for LSCM [Figure 2(d–f)], the images were slightly clearer when compared to when the dye used was FITC [Figure 2(a–c)] for the same hydrogel formulation. The differences in clarities of images obtained using the two dyes are best appreciated from color images (see Supporting Information Figure S2).

Scanning Electron Microscopy. As was seen for PHEMA sponges (containing no MeO-PEGMA), when P[HEMA-*co*-MeO-PEGMA] samples were dehydrated by RF-FD and then examined by SEM, prominent pores of dimensions 15–30 μm were seen [Figure 2(g–i)], and were assigned as artifacts due to formation of ice crystals during freezing. The droplet morphology apparent in the images obtained by confocal microscopy was evident in the SEM image of the 80 : 20 : 2 P[HEMA-*co*-MeO-PEGMA] sample. As the MeO-PEGMA content increased, the droplet morphology became increasingly distorted, and in the image of the 80 : 20 : 8 P[HEMA-*co*-MeO-PEGMA] sample, the droplets are almost totally coalesced, to give a morphology resembling a fibrous network [Figure 2(i)]. These distortions may be a consequence of the RF-FD process, but sample heating during deposition of a conductive graphite layer prior to SEM may also be a contributing factor, and we note that the distortion is greatest for the samples with the lowest *Tg* (see Figure S5 in Supporting Information for DSC curves of 80 : 20 : 5 and 80 : 20 : 8 polymers).

When PF-FD methods were used for each of the P[HEMA-*co*-MeO-PEGMA] sponge formulations, (80 : 20 : 2, 80 : 2 : 5, and 80 : 20 : 8) the morphologies of each sample looked similar to one another, but at the higher MeO-PEGMA concentrations the droplets were less well-defined [Figure 2(j–l)]. There was little evidence of large pores, a result that we attribute to the growth of only small (nm-scale) ice crystals during the plunge freezing process.[26] Critical point drying had little effect on the morphology as revealed by SEM for the P[HEMA-*co*-MeO-PEGMA] 80 : 20 : 2 and 80 : 20 : 5 samples [Figure 2(m,n)], but for the P[HEMA-*co*-MeO-PEGMA] 80 : 20 : 8 sample [Figure 2(o)], the morphology seen by SEM is significantly distorted, with droplets severely coalesced. This distortion is likely a consequence of the sample being heated above its *Tg* (sample $Tg < 35$°C—see Figure S5 in Supporting Information for the DSC curve for a 80 : 20 : 8 polymer formulation) during the critical

Applied Polymer SCIENCE

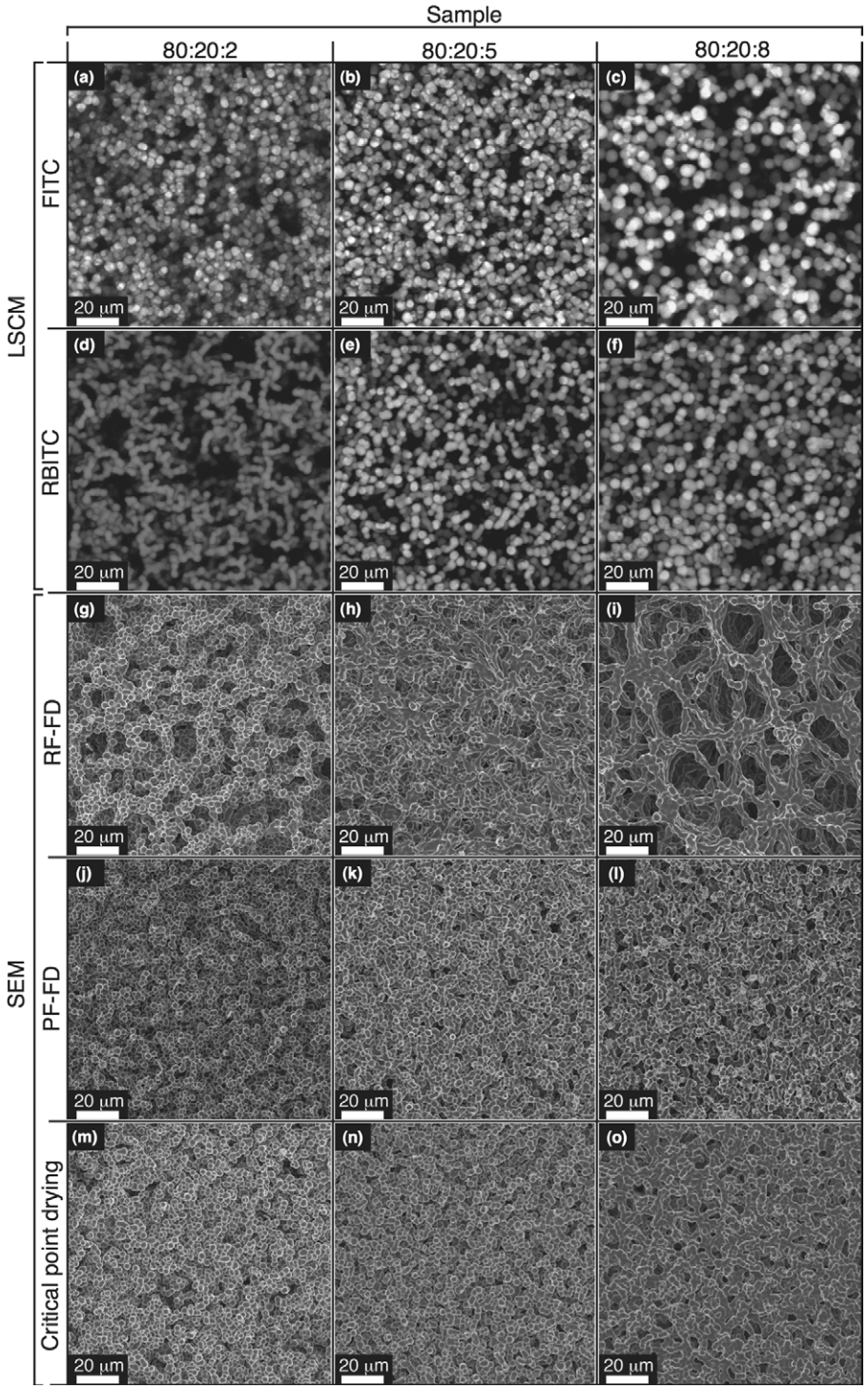

Figure 2. LSCM (a–f) and SEM (g–o) images of various P[HEMA-*co*-MeO-PEGMA] sponges. Samples imaged by LSCM were first labeled with either FITC or RBITC. Samples imaged by SEM were dried by RF-FD, PF-FD, or critical point drying. Colored LSCM images can be viewed in the Supporting Information Figure S2.

point drying process (which occurs at ca., 35°C). For all samples, the droplet features were slightly smaller in SEM images compared to their size in confocal microscopy images. This result is expected, since all samples shrunk by about 20% during the drying process. Although low-temperature methods gave the most accurate representation of the native morphology for SEM imaging, there were still discrepancies when compared to the images obtained from LSCM, suggesting LSCM is the only imaging method that reliably preserves the native morphology of P[HEMA-*co*-MeO-PEGMA] sponges.

Imaging P[HEMA-*co*-MeO-PEGMA] Homogeneous Gels

Laser Scanning Confocal Microscopy. When HEMA and MeO-PEGMA are copolymerized in water under conditions in which phase separation does not occur (H_2O : HEMA : MeO-PEGMA = 80 : 20 : 5 and 80 : 20 : 8), homogeneous gels are obtained. Intuitively, one might argue that the potential for artifacts to be induced during sample drying is greater for homogeneous gels, where all polymer chains are in intimate contact with a large concentration of water, compared to sponges having regions of hydrated polymer droplets and water-filled pores. When 80 : 20 : 5 and 80 : 20 : 8 P[HEMA-*co*-MeO-PEGMA] samples labeled with FITC were examined by LSCM [Figure 3(a,b)], very little morphological detail could be seen, as expected for homogenous gels. However, when RBITC was used as the labeling agent, LSCM images revealed surfaces covered with parallel lines [Figure 3(c,d)]. These lines are artifacts of the sectioning of the samples by the Vibratome, with the distance between the ridges being determined by the amplitude and the traverse speed of the cutting blade.

Scanning Electron Microscopy. When samples of 80 : 20 : 5 and 80 : 20 : 8 homogenous gels were subjected to RF-FD and then examined by SEM, the morphology revealed was grossly different to the "native" morphology seen by confocal microscopy. The SEM images displayed a "honeycomb" morphology with "pores" of approximately 75 μm [Figure 3(e,f)]. We tentatively suggest that the honeycomb morphology arises as a consequence of ice formation during the refrigerated-freezing process—as ice crystals form, polymer chains would be excluded from the growing ice domains, ending up as walls between ice crystals of random shapes and sizes, and removal of the ice during freeze-drying would leave the polymer walls as a honeycomb structure with voids left in place of the ice crystals. The RF-FD procedure caused the samples to change from flexible transparent materials to brittle opaque white materials, and was accompanied by some shrinkage of the samples, about 20% for the 80 : 20 : 5 formulation and 30% for the 80 : 20 : 8 formulation.

PF-FD is expected to be superior to RF-FD for drying P[HEMA-*co*-MeO-PEGMA] hydrogels due to its lesser propensity for formation of ice crystals, and therefore a reduced likelihood of inducing changes to the native morphology. When P[HEMA-*co*-MeO-PEGMA] hydrogels were examined by SEM after PF-FD [Figure 3(g,h)], the dominant features seen were the lines arising from the Vibratome sectioning procedure. Closer inspection of the images revealed the presence of small pores less that 1 μm in diameter for the 80 : 20 : 5 sample [Figure 3(g), inset] and 1–2 μm in diameter for the 80 : 20 : 8 sample [Figure 3(h)]. These small pores presumably arise as a consequence of formation of small crystals of ice during the rapid cooling of the samples, and because only small ice crystals are formed, the pores are much smaller than those in the samples dried by RF-FD.

Critical point drying requires temperatures to reach approximately 35°C. Since this temperature exceeds the *Tg* of the 80 : 20 : 5 and 80 : 20 : 8 P[HEMA-*co*-MeO-PEGMA] homogeneous gels, there is the possibility of increased molecular mobility during the supercritical drying process that may result in substantial changes to the native morphology. Once critically point dried, the P[HEMA-*co*-MeO-PEGMA] homogeneous gels had changed from transparent flexible materials to transparent but very stiff, glassy materials, and had undergone substantial shrinkage, to about 12–15% of their original volume (initial

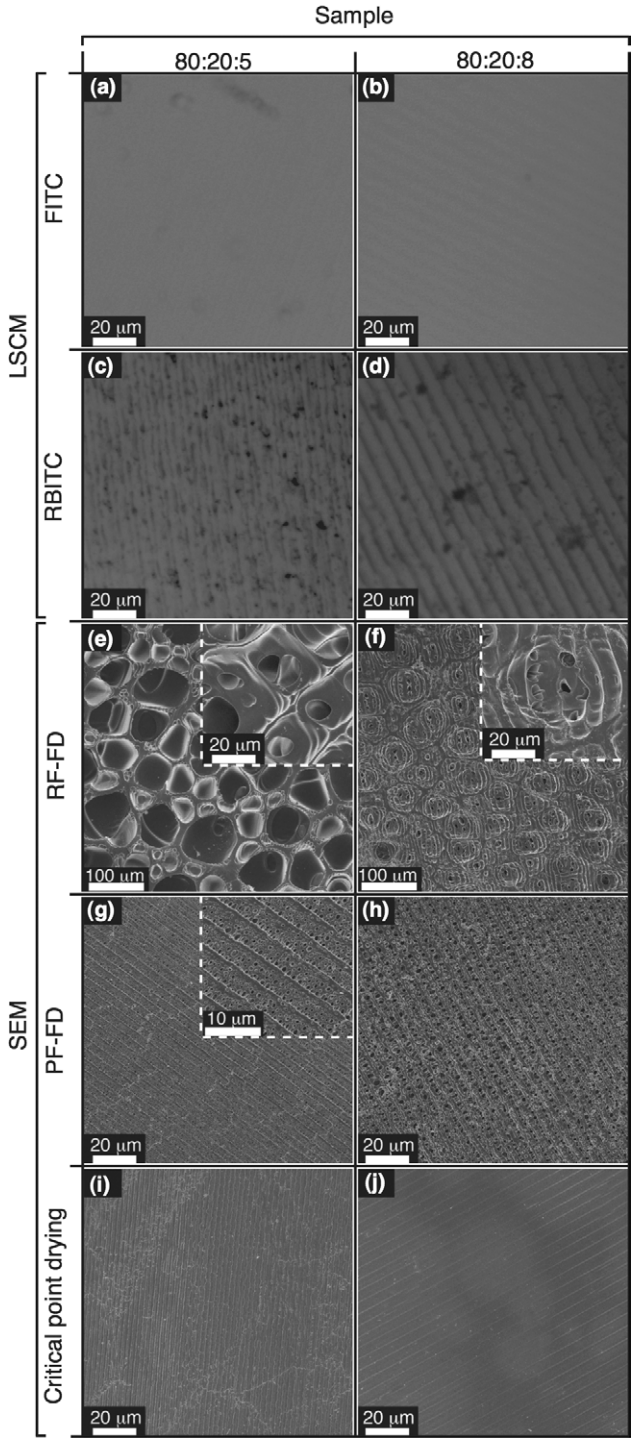

Figure 3. LSCM (a–d) and SEM (e–j) images of various P[HEMA-*co*-MeO-PEGMA] homogeneous gels. Samples imaged by LSCM were first labeled with either FITC or RBITC. Samples imaged by SEM were dried by RF-FD, PF-FD, or critical point drying. Colored LSCM images can be viewed in the Supporting Information Figure S3.

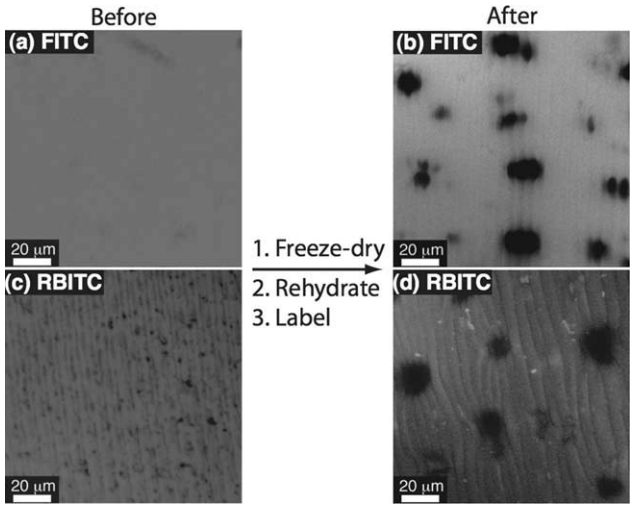

Figure 4. Before and after images of a 80 : 20 : 5 homogeneous gel that has been RF-FD, then rehydrated in water, and imaged via LSCM. Colored LSCM images can be viewed in the Supporting Information Figure S4.

dimensions 5 mm diameter, 300 μm thick; dimensions after critical point drying 3.2–3.5 mm diameter, 75–100 μm thick). Although this material must be different from the original hydrated homogeneous gel materials (it is dry, and therefore has a higher density of polymer chains making up for the loss of water), the SEM images for both samples do not reveal any significant morphological features [Figure 3(i,j)], as expected for homogeneous, non-porous glasses. The samples are scored by a series of parallel lines, artifacts formed during sectioning of the samples on the Vibratome. The similarity of spacing of the lines for these substantially shrunken samples compared to the "native" samples [Figure 3(a–d)] is a result of the sample disks shrinking primarily in the direction perpendicular to their circular faces rather than their edges.

We conducted a dehydration/rehydration experiment to determine whether the changes to the morphology of P[HEMA-*co*-MeO-PEGMA] hydrogels induced by RF-FD are irreversible. An 80 : 20 : 5 P[HEMA-*co*-MeO-PEGMA] sample that was dehydrated by RF-FD was rehydrated by soaking in water for 2 days, then cut into two pieces. Each piece was labeled with either FITC or RBITC and then imaged by LSCM. Both images clearly show large pores up to 30–40 μm in diameter [Figure 4(b,d)] not present in the original "native" morphology [Figure 4(a,c)]. The pores are smaller in the LSCM images than those seen in SEM images of a similar sample after RF-FD [Figure 3(d)]. Presumably, the large pores seen in the SEM image shrink during the rehydration process, as regions of polymer in the honeycomb walls [Figure 3(d)] absorb water and swell, but even after 2 days of rehydration (and additional time in aqueous dye solutions) is not able to remove all the pores formed during RF-FD. This result shows that the distortion of the native morphology during RF-FD is partly reversible, but the morphology of the hydrogel did not fully return to its native state.

CONCLUSIONS

Methods for preparation of PHEMA and P[HEMA-*co*-MeO-PEGMA] hydrogels for examination by LSCM do not involve sample drying or other procedures likely to significantly alter morphologies, and thus LSCM reveals the morphology of these materials in as close to their "native" state as is possible.

Artifacts arising during sample preparation (drying) of hydrogels resulted in SEM images showing morphologies that were often quite different from the native morphologies. Generally, RF-FD altered the native morphology of PHEMA and P[HEMA-*co*-MeO-PEGMA] hydrogels, due to the growth of crystals of water ice during freezing of the samples. Sample preparation by critical point drying was suitable only when the *Tg* of the sample was sufficiently higher than the temperature required for critical point drying; for samples having *Tg* below this temperature, critical point drying also caused significant changes to sample morphology. In most cases, PF-FD prior to SEM better preserved the native morphology for P(HEMA-*co*-MeO-PEGMA) sponges and gels, due to the lesser tendency for growth of ice crystals during the rapid freezing process, but nevertheless some artifacts were clearly evident in SEM images.

The work presented here has been limited to a study of PHEMA-based hydrogels, but the issues with sample preparation methods highlighted in our study are likely to arise with other hydrogels and similar systems. It is critical that researchers be aware of such issues when morphology is critical to the performance of a material in its intended application, for example when hydrogels are intended for use as scaffolds for tissue engineering.

ACKNOWLEDGMENTS

The authors acknowledge the Australian Research Council for funding (to M.V.B and T.V.C) and an Australian Postgraduate Award (to S.M.P). Y.S.C. thanks The University of Western Australia for a Jean Rogerson Postgraduate Fellowship and D.H.B thanks Curtin University of Technology for a Research and Teaching Fellowship. They would also like to thank John Murphy for his assistance with laser scanning confocal microscopy. They acknowledge the Australian Microscopy and Microanalysis Research Facility at the Centre of Microscopy, Characterization and Analysis, The University of Western Australia (a facility funded by The University of Western Australia, the Australian Government and the State Government of Western Australia) for providing access to facilities, and for scientific and technical assistance.

REFERENCES

1. Wichterele, O.; Lim, D. *Nature* **1960,** *185*, 117.
2. Chirila, T. V. *Biomaterials* **2001,** *22*, 3311.
3. Plant, G. W.; Harvey, A. R.; Chirila, T. V. *Brain Res.* **1995,** *671*, 119.
4. Plant, G. W.; Chirila, T. V.; Harvey, A. R. *Cell Transplant.* **1998,** *7*, 381.
5. Tsai, E. C.; Dalton, P. D.; Shoichet, M. S.; Tator, C. H. *Biomaterials* **2006,** *27*, 519.
6. Flynn, L.; Dalton, P. D.; Shoichet, M. S. *Biomaterials* **2003,** *24*, 4265.
7. Dalton, P. D.; Shoichet, M. S. *Biomaterials* **2001,** *22*, 2661.

8. Hicks, C. R.; Morris, I. T.; Vijayasekaran, S.; Fallon, M. J.; McAllister, J.; Clayton, A. B.; Chirila, T. V.; Crawford, G. J.; Constable, I. J. *Br. J. Ophthalmol.* **1999,** *83*, 616.
9. Chirila, T. V.; Chen, Y.-C.; Griffin, B. J.; Constable, I. *J. Polym. Int.* **1993,** *32*, 221.
10. Sharkawy, A. A.; Klitzman, B.; Truskey, G. A.; Reichert, W. M. *J. Biomed. Mater. Res. A* **1998,** *40*, 586.
11. Sharkawy, A. A.; Klitzman, B.; Truskey, G. A.; Reichert, W. M. *J. Biomed. Mater. Res. A* **1998,** *40*, 598.
12. Sharkawy, A. A.; Klitzman, B.; Truskey, G. A.; Reichert, W. M. *J. Biomed. Mater. Res. A* **1997,** *37*, 401.
13. Chirila, T. V.; Constable, I. J.; Crawford, G. J.; Vijayasekaran, S.; Thompson, D. E.; Chen, Y.-C.; Fletcher, W. A.; Griffin, B. J. *Biomaterials* **1993,** *14*, 26.
14. Cima, L. G.; Vacanti, J. P.; Vacanti, C.; Ingber, D.; Mooney, D.; Langer, R. *J. Biomed. Eng.* **1991,** *113*, 143.
15. Vacanti, J. P.; Morse, M. A.; Saltzman, W. M.; Domb, A. J.; Perez-Atayde, A.; Langer, R. *J. Pediatr. Surg.* **1988,** *23*, 3.
16. Fergg, F.; Keil, F. J.; Quader, H. *Colloid Polym. Sci.* **2001,** *279*, 61.
17. Hirokawa, Y.; Okamoto, T.; Kimishima, K.; Jinnai, H.; Koizumi, S.; Aizawa, K.; Hashimoto, T. *Macromolecules* **2008,** *41*, 8210.
18. Chalal, M.; Ehrburger-Dolle, F.; Morfin, I.; Vial, J.-C.; Aguilar de Armas, M.-R.; Roman, J. S.; Bölgen, N.; Piskin, E.; Ziane, O.; Casalegno, R. *Macromolecules* **2009,** *42*, 2749.
19. Miller, D. R.; Peppas, N. A. *Biomaterials* **1986,** *7*, 329.
20. Trieu, H. H.; Qutubuddin, S. *Colloid Polym. Sci.* **1994,** *272*, 329.
21. Baker, M. V.; Brown, D. H.; Casadio, Y. S.; Chirila, T. V. *Polymer* **2009,** *50*, 5918.
22. Liu, S.; Rachelee, P.; Ke, C.; Hedrick, J.; Yang, Y. *Biomaterials* **2009,** *30*, 1453.
23. Andac, M.; Plieva, F. M.; Denizli, A.; Galaev, I. Y.; Mattiasson, B. *Macromol. Chem. Phys.* **2008,** *209*, 577.
24. Savina, I. N.; Cnudde, V.; D'Hollander, S.; Hoorebeke, L. V.; Mattiasson, B.; Galaev, I. Y.; Prez, F. D. *Soft Matter* **2007,** *3*, 1176.
25. Dubochet, J. In Cellular Electron Microscopy, 1st ed.; McIntoch, J. R., Ed.; Academic Press: New York, **2007;** p 7.
26. Edelmann, L. In Handbook of Cryo-Preparation Methods for Electron Microscopy, 1st ed.; Cavalier, A., Spehner, D., Humbel, B. M., Eds.; CRC Press: Boca Raton, **2009,** p 367.